QUALITY ASSESSMENT OF INTERFEROMETRIC SAR DEMs

Michele CROSETTO*, Bruno CRIPPA**
* Joint Research Centre, Italy
Global Vegetation Monitoring Unit, Space Applications Institute
michele.crosetto@jrc.it
** Università degli Studi di Messina, Italy
bruno@ipmtf4.topo.polimi.it

KEY WORDS: Interferometric Procedure, DEM Generation, Image Coherence, Atmospheric Effects.

ABSTRACT

A new interferometric SAR (InSAR) procedure for DEM generation was employed to generate different DEMs from ERS SAR image pairs. The procedure was validated comparing the InSAR DEMs with a suited reference DEM. In the first part of the paper the principal features of the procedure are briefly summarised. The second part is focused on the quality assessment of the InSAR DEMs. They cover the same test area and come from one ascending SAR image pair, one descending pair and from the fusion of data coming from ascending and descending images. The analysis includes the influence of the SAR image coherence, the degradation of the DEM quality related to the terrain topography and the artefacts due to atmospheric effects.

1 INTRODUCTION

Interferometric SAR is a technique which allows to extract information on the terrain topography from the phase of the SAR signal. InSAR is based on the processing of complex SAR images acquired from slightly different points of view. A general review of the technique is given in (Gens and Van Genderen, 1996). It was applied for the first time at JPL (Jet Propulsion Laboratories) in 1986 using airborne data (Zebker and Goldstein, 1986). Today, a large number of research groups are working on DEM generation with InSAR data coming from different airborne and spaceborne systems. The importance of InSAR is related to its high spatial resolution, the good potential precision and the highly automated DEM generation capabilities.

About three years ago, five research groups (University of Thessaloniki, ICC - Cartographic Institute of Catalonia, ETH Zurich, Technical University of Graz and Polytechnic of Milan) joined in the frame of an European Union Concerted Action called ORFEAS (Optical-Radar sensor Fusion for Environmental ApplicationS). The purpose of the project was to assess the benefits of the integration (fusion) of data coming from different sources in orthoimage and DEM generation and land cover classification. A comprehensive data set, covering South Catalonia (Spain), was made available to ORFEAS participants by ICC. An important part of the ORFEAS project was devoted to the generation of DEMs using optical and SAR data. In this frame, the authors' activity at Polytechnic of Milan was focused on implementing a complete InSAR procedure for DEM generation, assessing the InSAR DEM quality and evaluating the pros and cons of the interferometric technique (validation).

In the following section, the main characteristics of our InSAR procedure are briefly described. For a comprehensive description of the procedure refer to (Crosetto, 2000). The second part of the paper is concerned with the analysis of the generated InSAR DEMs.

1.1 Interferometric SAR Procedure

The complete InSAR procedure we employ to generate DEMs, processing spaceborne (repeat-pass) data, consists of the following stages (Crosetto, 2000):

- image registration
- interferogram generation
- interferogram filtering
- coherence calculation
- phase unwrapping
- geometry calibration

- generation of the irregular grid of 3D points
- interpolation of the regular grid

The first three processing stages are based on the ISAR-Interferogram Generator software (distributed, free of charges, by ESA-ESRIN), an effective tool to obtain good filtered interferograms and the related coherence images (Koskinen, 1995). The phase unwrapping is based on the so-called "branch cuts" approach (Goldstein et al., 1988). The most original parts of the procedure are the rigorous model for the conversion from interferometric phases to terrain heights (used in the generation of the irregular grid of 3D points) and the calibration of the InSAR geometry (Crosetto and Crippa, 1999). The calibration is based on ground control points (GCPs), where either full GCPs or height GCPs may be used. It allows achieving an accurate geolocation of the InSAR generated DEMs. The implemented procedure allows fusing data coming from multiple InSAR pairs (e.g. ascending and descending pairs). In fact, it includes the simultaneous calibration of the geometry of different InSAR pairs based on the use of tie points (in full analogy with the procedures adopted in photogrammetry).

An important aspect of InSAR is the influence of atmospheric effects on the generated DEMs. These effects are mainly due to variations of atmospheric relative humidity between two SAR image acquisitions (Hanssen, 1998). They result in artefacts (e.g. depressions) in the generated InSAR DEMs interpreted as terrain relief. A single SAR pair can not check the presence of such artefacts, and this represents a very important limit of the InSAR technique. In order to reduce the influence of atmospheric artefacts, we adopt a strategy based on the use of auxiliary low-resolution height data (e.g. with a resolution 10 times lower the one of the InSAR DEMs), see (Crosetto, 2000). Firstly, the InSAR and auxiliary data are accurately geolocated with respect to the same reference system. The fusion procedure employs a multiresolution data analysis in the space domain adopting two resolution levels: the first one corresponds to the high frequency components of the terrain topography contained in the InSAR data and the second one corresponds to the low frequency components contained in the auxiliary data. The output DEM contains the high frequency components of the original InSAR DEM and the low frequency components (not affected by atmospheric effects) of the auxiliary data. The effectiveness of the atmospheric distortion compensation is shown in the analysis of the InSAR DEM quality.

2 ANALYSIS OF THE RESULTS

Over the ORFEAS test site different DEMs were generated using stereoscopic techniques (with SPOT and Radarsat stereo pairs) and InSAR procedures (ERS-1 interferometric pairs). The DEMs generated with our procedure were validated using a suited reference DEM (coming from aerial photogrammetry) whose precision is one order of magnitude better than that obtainable by InSAR DEMs. All DEMs analysed in the following cover the same area (approx. 25 by 35 km), which includes the flat plain crossed by the Ebro River and a set of mountain chains (the maximum height difference is about 1150 m). From the viewpoint of SAR images, this area includes many portions affected by foreshortening, layover and even shadow effects.

2.1 Ascending Image Pair

The characteristics of the ascending SAR image pair chosen for the processing are summarised in Table 1. The baseline length is about optimal for InSAR DEM generation and due to the quite high coherence a good interferometric phase quality can be expected. From the ascending pair we generated a 30 m spacing DEM that was compared with the reference one (see statistics of the processing type "without atmospheric corrections" in Table 2). The global bias (mean error) of the grid can be considered satisfactory, i.e. the calibration with 14 GCPs resolves quite well the geo-location of the generated 3D grid. One may notice an important decrease of the DEM precision between flat and mountainous areas (where unwrapping errors occur). In the following three important aspects of InSAR DEMs are discussed: the influence of the image coherence, the degradation of the DEM quality in mountainous areas and the atmospheric effects.

Acquisition Date	12 and 15 September 1991
Baseline Length	161.5 m
Sub-image range dimension	1500 pixels
Sub-image azimuth dimension	5000 pixels
Mean coherence of the SAR filtered images	0.57
InSAR geometry calibration	14 Ground Control Points

Table 1: Characteristics of the ERS-1 ascending InSAR pair.

Processing Type	Terrain type	Mean Error [m]	Standard Deviation [m]
Without Atmospheric Correction	hilly/flat	0.25	15.18
	mountainous	– 4.41	22.71
	entire area	**- 1.21**	**18.14**
Atmospheric Correction with Radargrammetry Data	hilly/flat	0.29	10.84
	mountainous	1.08	18.47
	entire area	**0.54**	**13.75**
Atmospheric Correction with Optical Data	hilly/flat	0.29	8.42
	mountainous	- 0.21	15.93
	entire area	**0.13**	**11.36**

Table 2: Ascending InSAR DEM results.

2.1.1 Image coherence. The coherence is a good indicator of the interferometric phase quality for DEM generation. Low coherence causes both the degradation of the precision of the InSAR point positioning and problems in the phase unwrapping. Therefore, in low coherence areas there is an important decrease of the DEM quality. In Figure 1 it is shown an example of low coherence area (along the Ebro River) with the corresponding large errors in the InSAR DEM. The decrease of DEM quality due to coherence is illustrated in Table 3, where the statistics of the height differences (InSAR versus reference DEM) computed for different coherence classes are reported. The standard deviation increases from 5 m (coherence 0.8÷1) to 18 m (coherence 0÷0.1).

The last row of Table 3 refers to the pixels of the geocoded coherence map that are not associated to any coherence value. These pixels are consequence of the slant range nature of SAR images that makes the terrain sampling very irregular. To these pixels (named “Interpolated” in Table 3) corresponds a large standard deviation (23.5 m).

2.1.2 Terrain Topography. There is a strong correlation between the type of terrain topography and the corresponding quality of the InSAR generated DEMs. Assumed to process images with a high mean coherence (e.g. bigger than 0.5), InSAR DEMs have quite good precision over areas characterised by gentle terrain variations. Dealing with complex terrain topography, some effects related to the SAR image distortions (foreshortening, layover and shadow) make difficult the phase unwrapping and result in spacing irregularities (i.e. “holes”) in the generated grids.

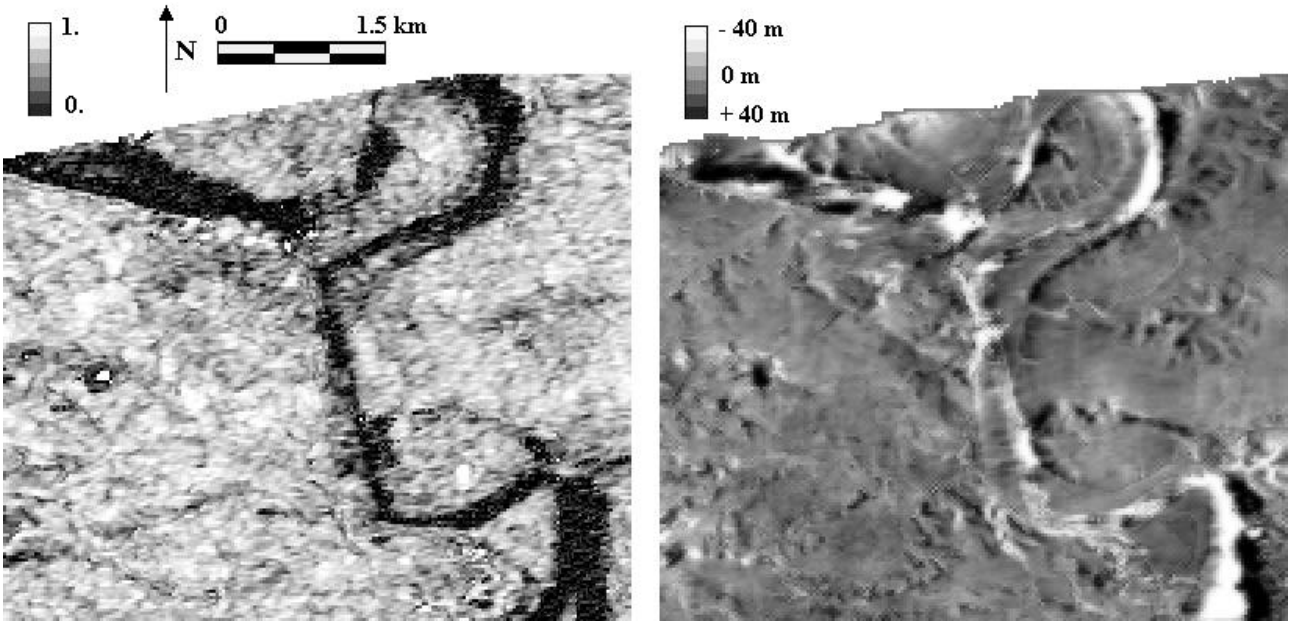

Figure 1: Ascending InSAR DEM. Geocoded coherence image (left) and the corresponding map of the height differences – InSAR versus reference DEM (right).

Coherence Range	Number of Pixels	Percentage [%]	Mean Error [m]	Standard Deviation [m]
0.8 ÷ 1.0	49183	7.8	0.34	5.01
0.7 ÷ 0.8	129600	20.7	0.34	6.13
0.6 ÷ 0.7	136767	21.8	0.66	8.06
0.5 ÷ 0.6	105632	16.8	0.93	10.37
0.4 ÷ 0.5	74602	11.9	0.77	12.95
0.3 ÷ 0.4	51289	8.2	- 0.36	15.22
0.2 ÷ 0.3	34206	5.5	- 1.47	17.11
0.1 ÷ 0.2	19663	3.1	- 2.30	17.76
0.0 ÷ 0.1	7874	1.3	- 3.01	17.96
Interpolated	18262	2.9	- 4.28	23.48

Table 3: Ascending InSAR DEM. Statistics of the height differences (InSAR versus reference DEM) computed for different coherence classes.

The extraction of height information is problematic especially in the terrain slopes facing the SAR antenna (see the slopes with positive values in Figure 2) where foreshortening and layover occur. As a consequence, InSAR DEMs are characterised by a peculiar feature: in the slopes facing the SAR antenna the DEM quality is severely degraded, while in those bent away from the SAR look direction the quality is higher (if the slopes are not in shadow). The decrease of DEM quality due to terrain topography is illustrated in Table 4, where the error statistics for different classes of slopes are reported. The quality decrease concerns both positive (i.e. facing the SAR antenna) and negative slopes, but comparing classes having the same absolute slope values one may notice an important difference in their standard deviations. For instance, the 33÷36 % class and the corresponding negative one have standard deviation of 22.5 m and 15.5 m respectively.

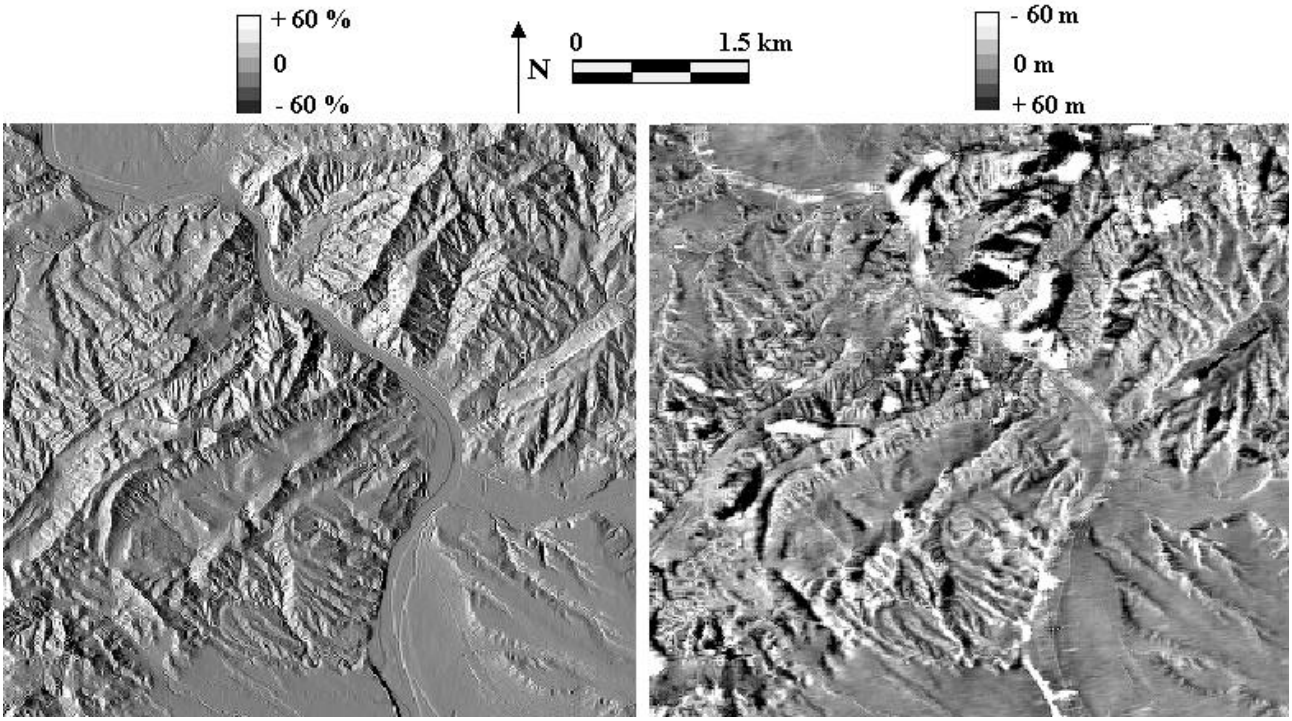

Figure 2: Ascending InSAR DEM. Map of the terrain slopes (left) and the corresponding map of the height differences – InSAR versus reference DEM (right). The slopes are calculated along the ground range direction, i.e. perpendicular to the satellite track. Slopes facing the SAR antenna have positive values.

Slope Range [%]	Number of pixels [%]	Standard Deviation [m]	Slope Range [%]	Number of pixels [%]	Standard Deviation [m]
0 ÷ 3	10.6	8.39	-3 ÷ 0	10.7	8.15
3 ÷ 6	9.2	9.02	-6 ÷ -3	9.3	8.18
6 ÷ 9	7.7	9.97	-9 ÷ -6	7.0	9.20
9 ÷ 12	5.7	11.01	-12 ÷ -9	5.3	9.91
12 ÷ 15	4.5	12.17	-15 ÷ -12	4.0	10.77
15 ÷ 18	3.5	13.30	-18 ÷ -15	3.1	11.46
18 ÷ 21	2.6	14.83	-21 ÷ -18	2.4	11.85
21 ÷ 24	2.0	16.23	-24 ÷ -21	1.9	12.05
24 ÷ 27	1.4	17.58	-27 ÷ -24	1.5	12.97
27 ÷ 30	1.0	19.01	-30 ÷ -27	1.1	13.71
30 ÷ 33	0.7	20.62	-33 ÷ -30	0.8	14.32
33 ÷ 36	0.5	22.53	-36 ÷ -33	0.6	15.53
> 36	1.2	24.41	< -36	1.6	19.53

Table 4: Ascending InSAR DEM. Statistics of the height differences (InSAR versus reference DEM) computed for different terrain slope classes. The slopes are calculated along the ground range direction, i.e. perpendicular to the satellite track. Slopes facing the SAR antenna have positive values.

2.1.3 Atmospheric effects. Atmospheric inhomogeneities during the SAR image acquisition cause distortion effects in the generated DEMs. Such effects, that are independent of the terrain topography and the coherence, can be noticed in the ascending DEM. In fact, it is affected by important systematic errors with low spatial frequency characteristics and magnitude up to 30÷35 m. The effect of such errors appears evident considering the autocovariance function of the height differences between the InSAR DEM and the reference one (see Figure 3). The correlation length is about 505 m and the correlation decreases to zero very slowly, i.e. the height differences are spatially highly correlated.

In order to assess the importance of atmospheric distortions, we adopted the data fusion procedure for atmospheric effect compensation described in (Crosetto and Pérez, 1999). We used as low resolution auxiliary data two coarse resolution grids (250 m spacing) of the ORFEAS data set generated using stereoscopic techniques (i.e. they are not affected by atmospheric effects). The first grid was interpolated from a 90 m DEM derived through a radargrammetric procedure implemented at ICC (Crosetto and Pérez, 1999) processing a pair of Radarsat images. The 90 m DEM has RMS error of 26.5 m (i.e. it is less precise and less dense than the InSAR DEM), but the errors are evenly distributed in the entire scene, i.e. they do not show systematic trends. This characteristic, confirmed by the correlation length of the height differences of about 40 m, is very important for the purpose of the data fusion procedure. The second grid used as auxiliary data is a DEM derived from optical images with 250 m spacing and RMS error of 23.1 m.

The two coarse resolution grids were fused separately with the ascending InSAR grid, obtaining two new DEMs (see the corresponding statistics in Table 2). Most of the systematic effects on the original InSAR DEM were properly removed through the data fusion. In both cases there is an important improvement of the DEM precision (the global standard deviation drops from 18.1 m to 13.8 and 11.4 m for radargrammetry and optical data respectively). The correlation length of the height differences (see Figure 3) is 55 m and 120 m for optical and radargrammetry data respectively. These values confirm the effectiveness of the artefact correction. In fact, the errors of the new DEM are almost spatially decorrelated because the systematic errors caused by atmospheric heterogeneity were properly removed. The atmospheric distortion compensation with optical data gives the best results due to the more homogeneous quality of the optical grid in the flat and mountainous areas.

2.2 Descending Image Pair

A pair of descending ERS-1 images covering the same area analysed in previous sections was processed (see Table 5). The low coherence of the filtered images (the mean over the entire scene is 0.41), due to the long time interval of the interferogram (35 days), made the phase unwrapping very difficult. Even with an image compression of two times in range and eight times in azimuth (pixel footprint size of about 32 by 40 m, while for the ascending images it was 16 by 20 m), only one third of the processed scene was correctly unwrapped. For the InSAR geometry refinement we adopted the joint calibration proposed in (Crosetto, 2000).

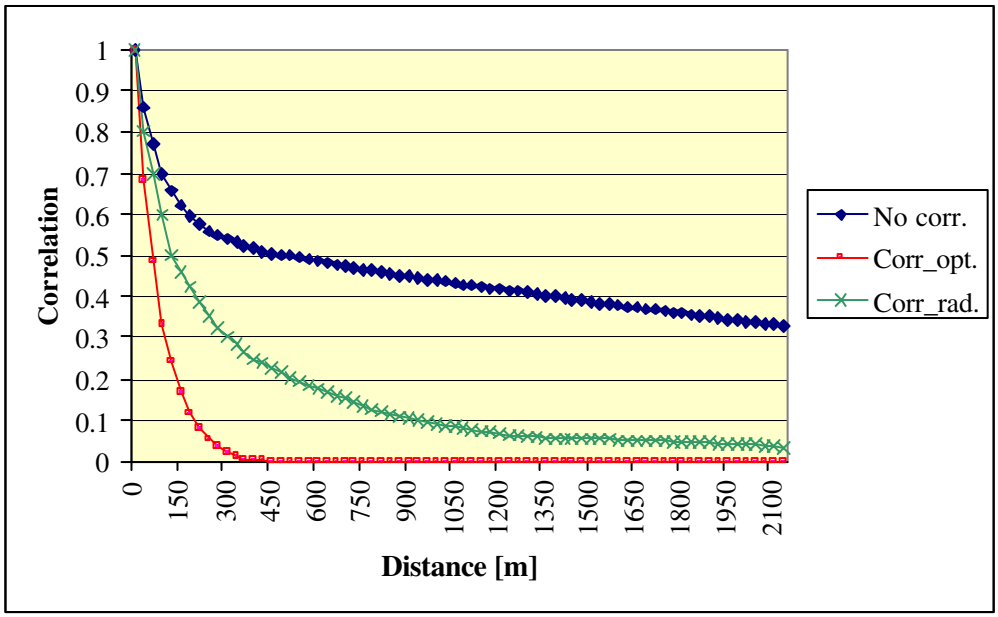

Figure 3: Ascending DEM. Autocovariance function of the height differences (InSAR versus reference DEM) for three grids: before correction of the atmospheric distortions ("No corr."), after correction with optical data ("Corr_opt.") and with radargrammetry data ("Corr_rad.").

In the overlapping area between ascending and descending images 8 tie points were collected. The joint calibration was performed using 14 GCPs for the ascending pair, 8 tie points and only 1 GCP for the descending pair. From the descending pair we generated a 60 m spacing DEM, that was compared with the reference one (see statistics of the processing type "without atmospheric corrections" in Table 6). The global bias (mean error) of the grid can be considered satisfactory, i.e. the joint calibration resolves quite well the geo-location of the generated 3D grid. There is an important decrease of the DEM precision in mountainous areas. The grid, compared with the ascending one described in section 2.1, has lower spatial resolution, covers only one third of the area and is less precise. These characteristics are related to the low coherence and to the high compression of the SAR images.

Acquisition Date	4 June and 9 July 1993
Baseline Length	160.7 m
Sub-image range dimension	1500 pixels
Sub-image azimuth dimension	5000 pixels
Mean coherence of the filtered images	0.41
InSAR geometry calibration	Ascending and Descending Joint Calibration: 14 GCPs Asc., 1 GCP Desc. and 8 Tie Points

Table 5: Characteristics of the ERS-1 descending InSAR pair.

Processing Type	Terrain type	Mean Error [m]	Standard Deviation [m]
Without Atmospheric Correction	hilly/flat	- 1.83	17.96
	mountainous	- 0.22	30.07
	entire area	**- 1.62**	**20.63**
Atmospheric Correction with Optical Data	hilly/flat	- 1.41	14.14
	mountainous	0.37	20.65
	entire area	**- 0.95**	**15.37**

Table 6: Descending InSAR DEM results.

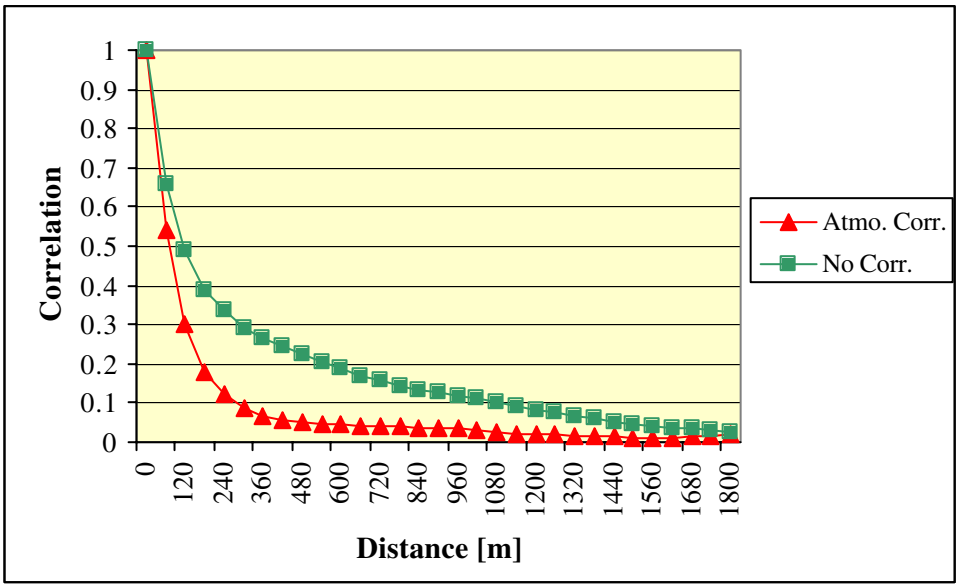

Figure 4: Descending DEM. Autocovariance function of the height differences (InSAR versus reference DEM) before correction of the atmospheric distortions ("No Corr.") and after correction using optical data ("Atmo. Corr.").

Terrain Type	Mean Error [m]	Standard Deviation [m]
hilly/flat	0.11	9.34
mountainous	- 0.28	16.56
entire area	**- 0.01**	**12.11**

Table 7: Ascending and descending data fusion DEM results.

Compared with the 30 m ascending grid, the 60 m descending one is less affected by atmospheric artefacts (the correlation length of the height differences is about 118 m, see Figure 4). We compensated for the atmospheric distortions in the descending grid using the 250 m DEM coming from optical images described in section 2.1.3. The new InSAR DEM was compared with the 60 m reference one (the relative statistics are reported in Table 6). The increase of the DEM precision (the global standard deviation drops from 20.9 m to 15.4 m) and the reduction of the correlation length from 118 m to 65 m indicate the effectiveness of the atmospheric effect correction.

2.3 Ascending and descending data fusion

In order to perform the data fusion, the ascending and descending grids have to be accurately geocoded with respect to the same reference system. The accurate relative geolocation was obtained through the joint InSAR geometry calibration based on GCPs and tie points. The ascending and descending grids were fused weighting each grid point according to its relative coherence (high weights are associated to points with high coherence). The DEM obtained by data fusion was compared with the reference one (see statistics in Table 7). The statistics refer to the entire area covered by the ascending DEM. In this area the fusion with descending data gives sensibly worse results than those obtained with the ascending grid alone. This is due to the very low quality of the descending data (low spatial resolution and much worse precision, compare the statistics in Tables 2 and 6) which is caused by the low coherence of the SAR images.

However, analysing more locally the data fusion DEM, its quality is higher than the ascending one in the slopes facing the ascending SAR antenna. In these areas, the ascending and descending grids have very different characteristics. For instance, considering a profile along one of such slopes (see Figure 5), the original descending irregular grid has an average sampling step of 23 m and a coherence of 0.52, while the ascending one has an average sampling step of 32 m and a coherence of 0.18. Along this profile the ascending grid shows huge height errors (due to aliasing errors and to low coherence), while the descending and data fusion profiles cope very well with the reference one. Despite the low quality of the employed descending InSAR data, this example confirms the effectiveness of the data fusion for areas affected by SAR image distortions (foreshortening and layover).

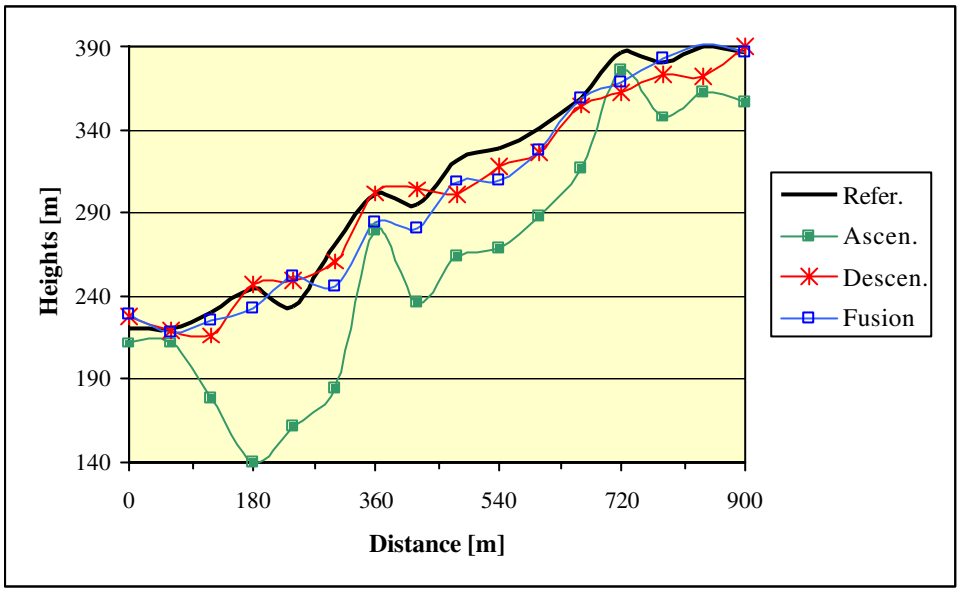

Figure 5: Data fusion DEM results. Analysis of a profile along a slope which faces the ascending SAR antenna.

3 CONCLUSIONS

A new InSAR procedure for DEM generation has been implemented. This procedure allows achieving an accurate geolocation of the generated grids and fusing data coming from multiple InSAR pairs. The analysis of the results showed strong correlation between DEM quality and image coherence, the degradation of the DEM quality in mountainous areas, and the importance of the atmospheric distortions. A suited strategy to reduce such distortions has been employed. In the analysed grids it increases considerably the DEM precision. The procedure has been tested deriving a DEM by ascending and descending data fusion. The data fusion gives good results in the areas affected by foreshortening and layover.

ACKNOWLEDGEMENTS

The authors thank Dr. Paolo Pasquali (now at RSL, University of Zurich) and Prof. Claudio Prati (from DEI, Polytechnic of Milan) for kindly providing the software for phase unwrapping, and Roman Arbiol and Fernando Pérez (from the Cartographic Institute of Catalonia) for providing the radargrammetric data used to compensate for the atmospheric effects.

REFERENCES

Crosetto, M., 2000. Calibration and validation of SAR interferometry for DEM generation. Paper submitted to the ISPRS Journal of Photogrammetry and Remote Sensing.

Crosetto, M., Crippa, B., 1999. Interferometric SAR calibration. Proceedings of the ISPRS - Commission VI Workshop, 15-19 February 1999, Parma (Italy), IAPRS, Vol. XXXII, Part 6W7, pp. 193-201.

Crosetto, M., Pérez, F., 1999. Radargrammetry and SAR interferometry for DEM generation: validation and data fusion. Proceedings of the CEOS SAR Workshop, CNES/ESA, Toulouse (France), 26-29 October 1999. Http://www.estec.esa.nl/CONFANNOUN/99b02/index.html.

Gens, R., Van Genderen, J.L., 1996. SAR interferometry – issues, techniques, applications. Int. J. Remote Sensing 17, (10), pp. 1803-1835.

Goldstein, R.M., Zebker, H.A., Werner, C.L., 1988. Satellite radar interferometry: two dimensional phase unwrapping. Radio Science 23, (4), 713-720.

Hanssen, R., 1998. Atmospheric heterogeneities in ERS tandem SAR interferometry. DEOS Report, No. 98.1, Delft University Press, Delft.

Koskinen, J., 1995. The ISAR-interferogram generator manual. ESA/ESRIN, Frascati, Italy.

Zebker, H.A., Goldstein, R.M., 1986. Topographic Mapping from Interferometric SAR Observations. Journal of Geophysical Research, Vol. 91, No. B5, pp. 4993-4999.